



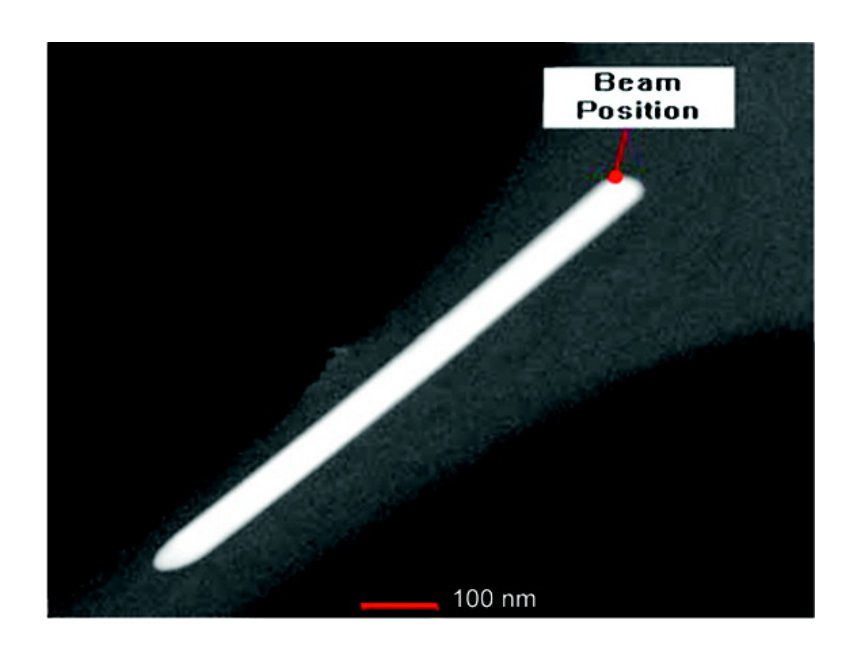
Letter

Single Particle Plasmon Spectroscopy of Silver Nanowires and Gold Nanorods

Moussa N#GomJan RingnaldaJohn F. MansfieldAshish Agarwal, and Nicholas KotovNestor J. ZaluzecTheodore B. Norris

Nano Lett., 2008, 8 (10), 3200-3204 • DOI: 10.1021/nl801504v • Publication Date (Web): 09 September 2008

Downloaded from http://pubs.acs.org on January 7, 2009



More About This Article

Additional resources and features associated with this article are available within the HTML version:

- Supporting Information
- Access to high resolution figures
- Links to articles and content related to this article
- Copyright permission to reproduce figures and/or text from this article

View the Full Text HTML



NANO LETTERS

2008 Vol. 8, No. 10 3200-3204

Single Particle Plasmon Spectroscopy of Silver Nanowires and Gold Nanorods

Moussa N'Gom*

Applied Physics Department and Center for Ultrafast Optical Sciences, University of Michigan, Ann Arbor, Michigan 48109

Jan Ringnalda

FEI Company, Hillsboro, Oregon 97124, and Fontana Laboratories, The Ohio State University, Columbus, Ohio 43210

John F. Mansfield

Electron Beam Analysis laboratory, University of Michigan, Ann Arbor, Michigan 48109

Ashish Agarwal and Nicholas Kotov

Chemical Engineering Department, University of Michigan, Ann Arbor, Michigan 48109

Nestor J. Zaluzec

Electron Microscopy Center, Argonne National Laboratory, Argonne, Illinois 60439

Theodore B. Norris

EECS Department and Center for Ultrafast Optical Sciences, University of Michigan, Ann Arbor, Michigan 48109

Received May 26, 2008; Revised Manuscript Received August 12, 2008

ABSTRACT

The excitation of surface plasmons in individual silver nanowires and gold nanorods is investigated by means of high-resolution electron energy loss spectroscopy in a transmission electron microscope. The transverse and longitudinal modes of these nanostructures are resolved, and the size variation of the plasmon peaks is studied. The effect of electromagnetic coupling between closely spaced nanoparticles is also observed. Finally, the relation between energy-loss measurements and optical spectroscopy of nanoparticle plasmon modes is discussed.

The surface plasmon modes of metallic nanoparticles lie in the optical (visible and near-infrared) part of the electromagnetic spectrum, corresponding to energies in the range of a few electronvolts. For this reason, optical spectroscopy has been one of the primary methods for investigating nanoparticle samples for many decades. Also, the development of new and powerful synthesis techniques has opened up the possibility of engineering the plasmon modes of metallic nanostructures for applications in optics and photonics. For example, the development of nanofabrication and

self-assembly based on wet chemistry methods has enabled synthesis of high yield gold (Au) and silver (Ag) colloidal particles with well-defined structures other than solid spheres,¹ including triangular prisms, disks,² shells,¹ wires,³ and rods.⁴ Most methods of synthesis produce samples with a range of nanoparticles with varying length and width. Characterization of samples in solution by optical absorption^{5,6} yields strongly inhomogeneously broadened spectra due to the sample polydispersity.

In order to overcome the inhomogeneous broadening inherent in ensemble measurements, single-particle spectra are desired. One of the primary challenges in optical studies

^{*} Corresponding author, mngom@umich.edu.

of nanostructures has been to measure the plasmon modes of single nanoparticles or single nanoparticle complexes. Scanning near-field optical microscopy (SNOM)⁷ and dark field illumination (DF)⁸ have been demonstrated to measure the absorption or scattering spectrum of a single nanoparticle. However, apart from the serious technical challenges involved in these experiments, SNOM and DF are limited in their ability to spatially resolve the mode structure of the plasmon, e.g., of a metal nanorod or nanowire. Thus, alternative techniques are required to measure the dielectric response function $\epsilon(\omega)$ of single metal nanoparticles.

Recent advances in electron microscopy have enabled the acquisition of energy loss spectra of single nanostructures with energies as low as 1.75 eV⁹ and 2.5 eV for metal clusters. Thus, the optical plasmon modes of nanoparticles are accessible using electron energy-loss spectroscopy (EELS). EELS involves analyzing the energy of initially monoenergetic electrons, after they have interacted with a specimen. This interaction takes place within a few atomic layers; hence EELS provides a highly localized spectrum of the excitations of the system. The electrons are then collected through a spectrometer to show their energy distribution following their interaction with the sample, thus providing information on the energy exchange with surface modes of the specimen.

Physically, a plasma oscillation may be induced either by the driving electric field of a resonant optical field or, impulsively, by the transient field associated with a fast electron passing near a nanoparticle. Energy lost by a monoenergetic electron beam due to excitation of plasmon oscillations can be directly measured, yielding the plasmon spectrum. Furthermore, the small size of the electron beam allows measurements of energy loss with high spatial resolution (1–4 nm), thus enabling the spatial structure of a plasmon mode to be mapped with a resolution not achievable by near-field optical methods.

The ability of high-resolution EELS to measure nanoplasmonic resonances has been demonstrated by Khan et al. 13 and the work of Colliex et al. 9 Those studies have shown the feasibility of detecting spectral features for low energy loss and of mapping the spatial variation of surface plasmon resonances on individual noble metal nanostructures. They have also demonstrated its capability to image these localized optical excitations with sufficient resolution to reveal dramatic spatial variation over a single nanoparticle. 9

The question naturally arises, therefore, as to the relation between optical spectroscopy and electron energy loss spectroscopy (EELS). The goal of both measurements is to determine the dielectric function of a nanoparticle or particle complex. Optical absorption generally measures $\text{Im}(\epsilon(\omega))$. On the other hand it has been established that the energy loss function characterizing energy transfer to the electron gas of bulk plasmon modes is determined by the energy loss function $\text{Im}(1/\epsilon_p(\omega))$. ¹⁴ EELS spectra for nanoparticles have been calculated directly for several specific cases. ^{15,16} In this Letter, we compare the spectra obtained by optical absorption and by EELS to observe the relationship between these different approaches to plasmon spectroscopy.

Using state-of-the-art EELS in the various TEMs used in this work, we have resolved the plasmon modes of individual Ag nanowires and individual and pairs of Au nanorods. These particles have plasmon resonances in the UV, visible, and near-infrared regions. They have two plasmon absorption resonances; one is due to the transverse oscillation of electrons (i.e., electron motion perpendicular to the long axis of the rods or wires) with energy around 2.5 eV for gold and 3.5 eV for silver, approximately coincident with the plasmon of spherical particles, while the second plasmon is due to the oscillation of electrons along the long axis. This longitudinal mode is red-shifted and strongly depends on the nanostructure as the length divided by the width of the nanoparticle.⁵ The energy resolution of the EELS system is sufficient to spectrally resolve these two modes. Furthermore, utilizing the nanoscale dimensions of the focused electron beam of the TEM, we are able to excite the nanoparticles at precise locations and thus probe the spatial dependence of the relative excitation of the different plasmon modes. Energy loss measurements reported herein were recorded in a stationary probe mode.

Au nanorods were fabricated using a seeding growth method to make gold nanorods^{4,17} with varied aspect ratio. The gold particle aspect ratio could be controlled from 1 to 7 by simply varying the ratio of seed to metal salt in the presence of a rodlike micellar template.¹⁸ The Ag nanowires were assembled using the polyol method; details are given in ref 19.

EELS measurements were carried out on an FEI Titan (OSU), FEI Tecnai F20 (ANL), and a JEOL 2010 (UofM) all equipped with high-resolution EELS (HREELS) spectrometers with energy resolutions ranging from 0.2 to 1 eV. To improve the visibility of the spectral features in the EELS data presented in this work, deconvolution was performed using the Richardson—Lucy algorithm.²⁰ The nanoparticle spectra were deconvoluted from the spectrum of the support film collected under similar conditions. We note however that our conclusions regarding resonance positions and behavior are not dependent on the deconvolution.

A single droplet of the solution of Au or Ag nanostructures diluted in deionized water was placed on a thin SiO_x film supported on a 3 mm diameter copper mesh TEM grid. The solvent was evaporated in room temperature. Care was taken when acquiring single-nanoparticle spectra to leave sufficient spatial separation between particles to avoid electromagnetic coupling. After identifying a nanostructure of interest, we positioned the beam at the corner of the particle to induce charge displacement along both axes of the wire. Figure 1b shows raw and deconvoluted EEL spectra taken at the corner of a Ag nanowire 706 nm long and 50 nm wide (Figure 1a). Two main surface plasmon peaks are identified, at 1.8 and 3.54 eV, which correspond to the longitudinal and transverse plasmons, respectively. For comparison, the optical absorption spectrum of the solution is shown in Figure 2; the peak at 3.5 eV corresponds to the transverse plasmon absorption and the broad peak at lower energy is due to the absorption of different length and shape nanostructures present in the solution. The extremely broad peak in the ensemble optical

Nano Lett., Vol. 8, No. 10, **2008**

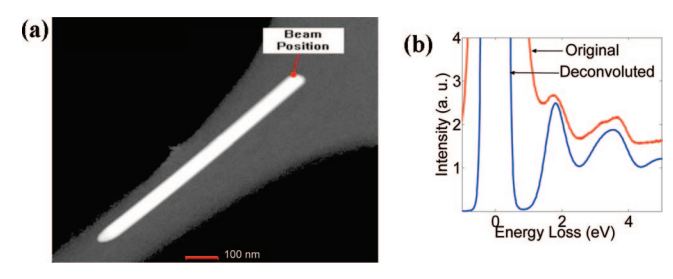


Figure 1. (a) TEM image of Ag nanowire of length 706 nm and width 50 nm. (b) Deconvoluted spectrum acquired from the edge of the particle. Two peaks are clearly resolved; the transverse mode is at 3.54 eV and longitudinal mode is at 1.8 eV.

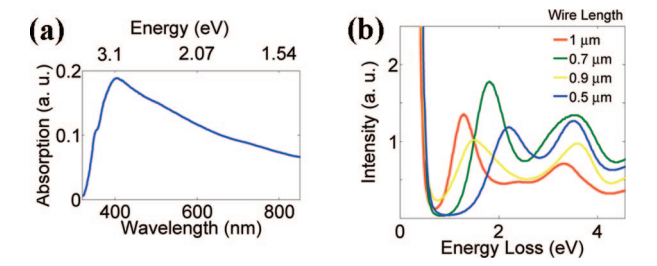
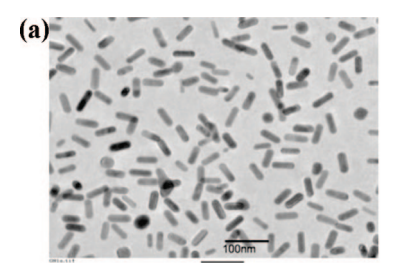


Figure 2. (a) Ensemble optical absorption spectrum of Ag nanowires in solution. The peak at 3.5 eV is due to the transverse plasmon absorption. The broad peak is due to longitudinal plasmon absorption; the broadening is due to contributions from different length and width nanowires present in the solution. (b) Deconvoluted spectra of four different length Ag wires: the transverse plasmon resonance is relatively consistent (3.4–3.6 eV). The slight peak variations can be largely attributed to wire thickness and film support. The longitudinal plasmon peak is red-shifted as the wire length increases confirming its dependence on the particle aspect ratio.

spectrum implies a highly polydisperse sample, containing nanostructures with a wide range of aspect ratios.^{21,22} We note that the nanoparticle concentration in solution is very low, and surface charge prevents aggregation, so the breadth of the spectrum may be attributed to inhomogeneous broadening and not to random interparticle electromagnetic coupling.

Figure 2(b) shows spectra taken from different nanowires of varying length and width, accurately measured from the TEM image to within a nanometer. As the length of the nanowire increases, we observe a significant shift to lower energy of the longitudinal plasmon peak, while the transverse plasmon peak is nearly constant. The slight variation in the transverse mode peaks is due to different nanowire width and support film thickness. The variation of mode energy with nanowire dimensions implies strong inhomogeneous broadening of the optical absorption spectra of ensembles; the optical absorption of our Ag nanowire sample is shown in Figure 2a. Theory predicts that the number of resonance peaks increases when the symmetry of the cross sections of the Ag nanowires decreases.²³ Our results for 2D nanoparticles (nanowires) clearly show the longitudinal plasmon blue-shifted as the particle aspect ratio decreases. This result has been demonstrated optically in ensemble spectra, where the absorption spectra of nanowire samples fabricated with different average length.²⁴



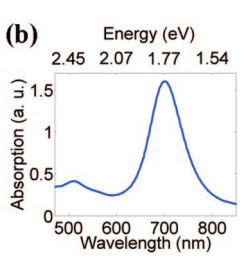


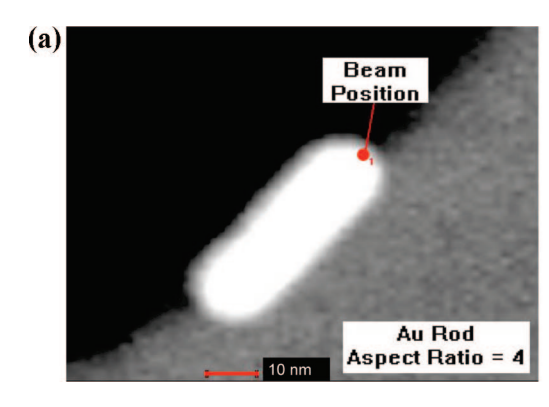
Figure 3. (a) An overview of the different size and shape Au nanorods present in the sample. The solution is mainly composed of different size nanorods. (b) Ensemble optical absorption spectrum of solution. The first peak at 520 nm is the main surface plasmon absorption of Au and the second is to the longitudinal absorption of the nanorods. The observed broadening is due to the polydispersity of the sample.

We next consider the plasmon resonances of Au nanorods which are generally at lower energy than those of silver. Figure 3a shows an overview of the shape and size of the nanorods present in the solution that accounts for the two peaks in the optical absorption spectrum in Figure 3b. The plasmon peak at 520 nm (2.4 eV) is the transverse plasmon mode for Au nanorods and is present in spherical particles at the same energy. The much broader peak is due to the longitudinal modes, with wavelength maximum depending on the aspect ratio. To obtain a single-nanoparticle spectrum, we selected a nanorod 40 nm long and 10 nm wide; again the electron beam was positioned at the edge of the rod, as shown in Figure 4a to induce charge oscillations along the axes of the rod. Figure 4b shows the resulting spectrum; the longitudinal plasmon resonance maximum is located at 1.74 eV corresponding to the theoretical value of an AR equal to 4;6 the transverse plasmon mode is located at 2.47 eV.

Metal nanoparticle plasmon modes can also be affected by near-field interparticle coupling.^{25,26} Figure 5a shows two nanorods separated by a 10 nm gap. We measured the energy loss in the gap and at the edge of the particles at close proximity; deconvoluted spectra are shown in Figure 5b.

Previous investigations^{25–27} have shown that the plasmon resonance of two electromagnetically coupled particles is shifted to lower frequencies or lower energy. The peak shift dependence on particle proximity can be interpreted by a simple dipole-dipole interaction. The spectra in Figure 5b show that the resonance peak is red-shifted when the particle is excited at the edge of either rod. This shift is due to the weakened restoring forces on the oscillating charge: the electron beam at one edge pushes the negative charges toward the other edge. These negative charges in turn induce the same effect on the second nanorod. Thus negative charges near the gap face positive charges, effectively lessening the net restoring effect and shifting the mode to lower energy. When the electron beam is positioned in the gap between the two particles, the energy loss peak amplitude is slightly larger, which may be due to local field enhancement. Additionally, we see that the peak is slightly blue-shifted relative to excitation at the edge. This is attributed to the increased restoring force present with excitation in the gap, although microscopic calculations of the EELS spectra for

3202 Nano Lett., Vol. 8, No. 10, 2008



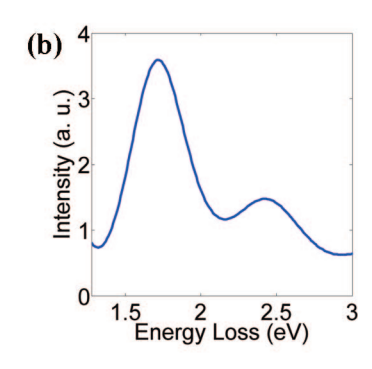
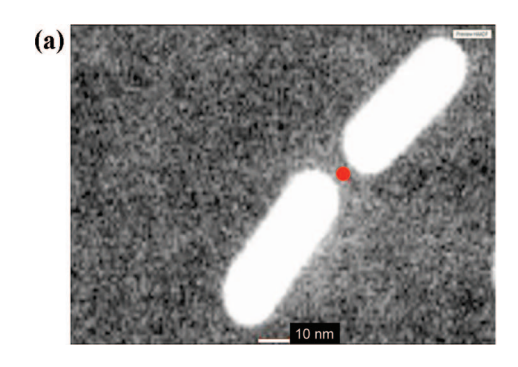


Figure 4. (a) TEM image of a single Au rod 40 nm long and 10 nm wide with electron beam position indicated by the small red circle a the tip of the particle. (b) Deconvoluted Spectrum of a single nanorod. Both plasmon peaks are resolved: the longitudinal plasmon peak is at 1.74 eV and the transverse peak is at 2.47 eV.



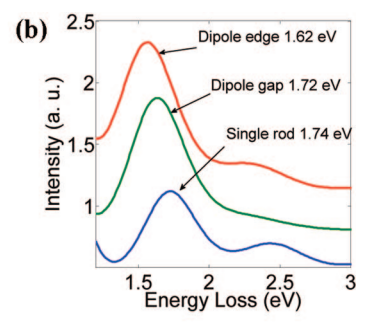


Figure 5. (a) Two nanorods (dipole) positioned with a 10 nm gap. (b) Deconvoluted spectra of the dipole taken at the edge and in the gap between the two rods along with that of the single nanorod Figure 4b. The plasmon peak at the edge of the dipole is 1.62 and 1.72 eV. In the gap both peaks are red-shifted compared to the single rod plasmon peak, but the shift is smaller for excitation in the gap.

coupled nanoparticles is required for a detailed understanding of the peak shifts.

We now turn to a discussion of the relation between EEL spectra and optical measurements. Pines and Bohm²⁸ first suggested that the energy losses suffered by electrons passing near or through a small metallic object are due to the excitation of surface plasmons. Subsequent theoretical work addressed energy loss in thin films,¹² metallic spheroids (sufficiently small that retardation effects may be neglected),¹⁶ and fully relativistic calculations of energy loss.¹⁵ In order to interpret our experiments, we consider the nanowires and nanorods to be reasonably approximated as prolate spheroids of varying aspect ratio.

Our aim here is to compare energy loss spectra calculated from $\text{Im}(1/\epsilon_p(\omega))$ and from the analytical energy loss probability calculated for prolate spheroids and to relate these to optical absorption spectra.

We begin with the imaginary part of the inverse dielectric function 14 —the loss function $\mathrm{Im}(1/\epsilon_p(\omega))$ —where the frequency-dependent dielectric function $\epsilon_p(\omega)$ of the prolate spheroid is derived using the electrostatic approximation 29 as detailed by Bohren. 30 The dielectric function of a prolate spheroid can be expressed as

$$\epsilon_p \sim 1 + \alpha$$
 (1)

where α is the polarizability of the prolate particle; see ref 30 and references therein. We take the energy loss probability derived by Ferrell et al. (see eq 13 in ref 16) for an electron with constant velocity v and impact parameter b passing a

prolate spheroid traveling parallel its minor axis

$$\Gamma_{\text{loss}}(\omega) = \frac{2}{\nu \omega} \sum_{l=1}^{\infty} \sum_{m=0}^{l} C_{lm} \frac{P_{lm}(\eta_o)}{Q_{lm}(\eta_o)} J_{l+1/2} \left(\frac{a\omega}{\nu}\right) K_m^2 \left(\frac{b\omega}{\nu}\right) \times \operatorname{Im}\left[\alpha_{lm}(\omega)\right] \quad (2)$$

where a is the focal length of the confocal spheroid, η_o depends on the aspect ratio ρ of the particle and is given by

$$\eta_o = \frac{1}{\sqrt{\rho^2 - 1}}$$

 $\text{Im}[\alpha_{lm}(\omega)]$ is the imaginary part of $\alpha_{lm}(\omega)$

$$\alpha_{lm}(\omega) = \frac{\epsilon(\omega) - 1 - [\epsilon_m(\omega) - 1]\beta_{lm}}{\epsilon(\omega) - \epsilon_m(\omega)\beta_{lm}}$$

and

$$C_{lm} = (-1)^m (2 - \delta_{0m})(2l + 1)$$

with, $\delta_{0m} = 1$ if m = 0 or 0 for $m \neq 0$.

Finally

$$\beta_{lm} = \frac{Q'_{lm}(\eta_o) P_{lm}(\eta_o)}{P'_{lm}(\eta_o) Q_{lm}(\eta_o)}$$
(3)

is the surface plasmon eigenvalue for the (l, m) mode of the dielectric function and real and negative number, P_{lm} and Q_{lm} are the associated Legendre functions of the first and second kinds, respectively; $J_{l+1/2}$ is a the ordinary Bessel function of order l+1/2, and K_m is the modified Bessel function of order m.

Nano Lett., Vol. 8, No. 10, **2008**

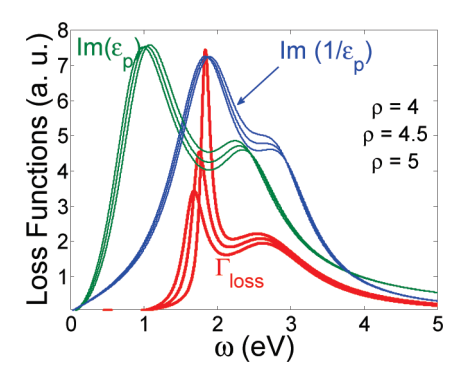


Figure 6. Comparison between analytical representations of the energy loss peak for three Au prolate spheroids. For all expressions we set the host dielectric $\epsilon_m = 1$ and the damping coefficient for the Drude model for dielectric $\gamma = 1.06$. The aspect ratio ρ is varied to show its influence on the plasmon peak absorption.

In Figure 6, we plot together the optical absorption of the prolate spheroid here taken as^{29,30}

$$Im(1+\alpha) \tag{4}$$

for the transverse and longitudinal axis, the energy loss probability equation from (2) and the size dependent Im(1/ $\epsilon_p(\omega)$). The medium dielectric is kept constant ($\epsilon_m=1$), and the Drude dielectric function

$$\epsilon(\omega) = 1 - \frac{\omega_p^2}{\omega(\omega + i\gamma)}$$

has been used for the material response. Although in principle the interband contribution to the dielectric constant for Au should be included, the Drude model does give a very good approximation to the Au plasma frequency since the free-carrier contribution is much larger than the interband part of the dielectric constant, as indicated by Dressel and Grüner.³¹ We have selected parameters appropriate for Au ($\omega_p = 2.5 \text{ eV}$, $\gamma = 1.06$), the effect of the aspect ratio is shown ($\rho = 4$, 4.5, and 5). Atomic units are used (a.u., i.e., $e = m = \hbar = 1$).

It is apparent in Figure 6 that the EELS and optical measurements are sensitive to the same modes, and each clearly resolves the longitudinal and transverse modes of the structures. Furthermore, the red shift of the longitudinal plasmon peak with increasing aspect ratio is also manifested in all three approaches. Nevertheless, important differences are apparent. The spectral peak position of the optical absorption $\text{Im}(\epsilon_p)$, the loss function $\text{Im}(1/\epsilon_p)$, and the loss probability Γ_{loss} , do not exactly coincide. The loss function and the loss probability longitudinal peaks are blue-shifted relative to the longitudinal peak of the optical absorption. Their transverse peaks also show less dependence on the aspect ratio than the transverse optical absorption peak. The energy loss expressions $\Gamma_{\rm loss}(\omega)$, and ${\rm Im}(1/\epsilon_p(\omega))$ for a prolate spheroid with $\rho = 4$, show longitudinal peaks at 1.6 and 1.76 eV, respectively, and transverse peak between 2.4 and 2.5 eV. These values agree quite well with our experimental values for the Au nanorod with the same ρ displayed in Figure 4b.

The primary consequence of this work is that the dielectric function of metallic nanostructures can be deduced from an EELS experiment, and the mode structure required for understanding or engineering optical plasmonic interactions can be accomplished through EELS measurements of single nanoparticles.

Acknowledgment. The authors acknowledge Professor Hamish Fraser from The Ohio State University for the use of the probe-corrected monochromated Titan System with 866 GIF. This work was carried out in part at the University of Michigan Electron Beam Analysis laboratory (EMAL), The Ohio State University Fontana Laboratory, and the Electron Microscopy Center for Materials Research at Argonne National Laboratory, a U.S. Department of Energy Office of Science Laboratory operated under Contract No. DE-AC02-06CH11357 by UChicago Argonne, LLC. Ashish Agarwal and Nicholas Kotov acknowledge the support by the AFOSR under MURI Grant FA9550-06-1-0337.

References

- (1) Hao, E.; Li, S.; Bailey, R. C.; Zou, S.; Schatz, G. C.; Hupp, J. T. *J. Phys. Chem. B* **2004**, *108*, 1224–1229.
- (2) Mock, J. J.; et al. J. Chem. B 2002, 116 (15),
- (3) Graff, A.; Wagner, D.; Ditlbacher, H.; Kreibig, U. Eur. Phys. J. D 2005, 34, 263–269.
- (4) Jana, N. R.; Murphy, C. J. Adv. Mater. 2002, 14 (1)), 8082.
- (5) Link, S; El-Sayed, M. A. Spectral properties and relaxation dynamics of surface plasmon electronic oscillations in gold and silver nanodots and nanorods. J. Phys. Chem. B 1999, 103, 8410–8426.
- (6) Susie, Eustis; Mostafa A., El-Sayed J. Appl. Phys. 2006, 100, 044324.
- (7) Klar, T.; Perner, M.; Grosse, S.; von Plessen, G.; Spirkl, W.; Feldman, J. Phys. Rev. Lett. 1998, 80 (19), 4249–4252.
- (8) Sönnichsen, C.; Franzl, T.; Wilk, T.; von Plessen, G.; Feldman, J.; Wilson, O.; Mulvaney, P. Phys. Rev. Lett. 2002, 88 (7), 077402.
- Nelayah, J.; Kociak, M.; Staphan, O.; Garcia de Abajo, F. J.; Tencio, M.; Henrard, L.; Taverna, D.; Pastoriza-Santos, I.; Liz-Marzin, L. M.; Colliex, C. Nat. Phys. 2007, 3, 348–353.
- (10) Batson, P. E. Surface Plasmon in Cluster of Small Spheres. Phys. Rev. Lett. 1982, 49 (13), 936.
- (11) Egerton, R. F. Electron Energy Loss Spectroscopy in the Electron Microscope, 2nd ed; Plenum Press: New York and London, 1996.
- (12) Ritchie, R. H. *Phys. Rev.* **1957**, *106* (5), 874–881.
- (13) Khan, I. R. Faraday Discuss. 2006, 132, 171178.
- (14) Pines, D. Elementary Excitations in Solids: Lectures on Phonons, Electrons, and Plasmons; W.A. Benjamin, Inc.: New York, 1964.
- (15) Garcia de Abajo, F. J.; Howie, A. Phys. Rev. Lett. 1998, 80 (23), 5180.
- (16) Illman, B. L.; Anderson, V. E.; Warmack, R. J.; Ferrell, T. L. Phys. Rev. B 1988, 38 (5), 3045.
- (17) Jana, N. R. Chem. Commun. 2001, 617.
- (18) Nikhil, R. J. Phys. Chem. B 2001, 105, 4065-4067.
- (19) Korte, Kylee National Nanotechnology Infrastructure Network (2007 REU Research Accomplishments); 2007; p 28.
- (20) Gloter, A. Ultramicroscopy 2003, 96, 385-400.
- (21) Qui, Le; et al. IEEE J. Sel. Top. Quantum Electron.) 2007, 13 (6),
- (22) Erni, R.; Browning, N. D., *Ultramicroscopy* **2007**, *107*, 267–273.
- (23) Kottman, J. P.; Martin, O. J.; Smith, D. R.; Schultz, S. *Phys. Rev. B* 2001, 64, 235402.
- (24) Gao, Y.; Song, L.; Jiang, P.; Liu, L. F.; Yan, X. Q.; Zhou, Z. P.; Liu, D. F.; Wang, J. X.; Yuan, H. J.; Zhang, Z. X.; Zhao, X. W.; Dou, X. Y.; Zhou, W. Y.; Wang, G.; Xie, S. S.; Chen, H. Y.; Li, J. Q. J. Cryst. Growth 2005, 276, 606–612.
- (25) Su, K. H.; Wei, Q.-H.; Zhang, X.; Mock, J. J.; Smith, D. R.; Schultz, S. Nano Lett. 2003, 3 (8), 1087.
- (26) Rechberger, W.; et al. Optical properties of two interacting particles. Opt. Commun. 2003, 220, 137.
- (27) Quinten, M.; et al. Optical absorption of pairs of small metal particles. Surf. Sci. 1985, 156, 741.
- (28) Pines, D.; Bohm, D. Phys. Rev. 1952, 85 (338),
- (29) Jackson, J. D. Classical Eletrodynamics, 3rd ed.; John Wiley & Sons, Inc.: New York, 1998.
- (30) Bohren; Craig F.; Human, Donald Absorption and Scattering of Light by Small Particles, 1st ed.; John Wiley & Sons, Inc.: New York, 1998.
- (31) Dressel, Martin; Grüner, George Electrodynamics of Solids; Crambridge University Press: Cambridge, MA, 2002.

NL801504V